Supporting Information

Enabling Active Defect Healing via Lateral Spread Growth for Highly Reversible Zinc Anodes

Yiping Wang, Yanfeng Li, Yang Jin*, Yun Yin, Ming Chen, Jun Li

Y. Wang, Y. Jin, Y. Yin, M Chen, J. Li

Engineering Research Center of Comprehensive Utilization and Clean Processing of Phosphorus Resources, School of Chemical Engineering, Sichuan University

Chengdu, Sichuan 610065, China

E-mail: jinyangyoung@126.com, jinyangyoung@scu.edu.cn

Y. Li

SINOPEC Nanjing Engineering Co., Ltd., No. 16 Xianlin Avenue, Qixia District

Nanjing, Jiangsu 210049, China

Experimental Section

Chemicals

Zinc sulfate heptahydrate ($ZnSO_4 \cdot 7H_2O$, 99.5%, Innochem), dibutyl phosphate (DBP, 97%, Adamas), sodium hydroxide (NaOH, AR, Chengdu Kelong Chemical Co., Ltd.), vanadium pentoxide (V_2O_5, AR, Aladdin), sodium chloride (NaCl, AR, Chengdu Kelong Chemical Co., Ltd.), acetylene black (AR, Cyber Electrochemical Materials), NMP (99.5%, Aladdin), and PVDF (AR, Cyber Electrochemical Materials) were all used without further purification.

Preparation of electrolytes and electrodes

The 2 M $ZnSO_4$ base electrolyte (ZSO) was prepared by dissolving $ZnSO_4 \cdot 7H_2O$ in deionized (DI) water. To obtain the optimized electrolyte (ZSO+DBP), DBP was added to the ZSO solution to achieve a concentration of 20 mM. Since the functional hydroxyl groups of DBP render it slightly acidic, trace amounts of dilute NaOH solution were used to precisely adjust the pH of the composite electrolyte to match that of the ZSO electrolyte. This strict pH control guarantees that the subsequent electrochemical enhancements are exclusively ascribed to the interfacial regulation of the DBP molecules.

Zn foils with a thickness of 100 μm were punched into discs with a diameter of 14 mm to serve as Zn electrodes for Zn||Zn symmetric cells, Zn||Cu half cells, and full cells.

2 g V_2O_5 was added into 60 mL of 2 M NaCl solution and stirred at room temperature for 72 h before centrifugation. The collected solid was washed several times alternately with deionized (DI) water and anhydrous ethanol. Finally, the product was dried at 60 °C for 12 h to obtain NaV_3O_8 (denoted as NaVO).

PVDF was dissolved in NMP to yield a solution with a mass fraction of 4%. NaVO, acetylene black, and PVDF were mixed homogeneously at a weight ratio of 6:3:1. The resulting slurry was coated onto hydrophilic carbon paper and dried at 60 °C under vacuum for 6 h to obtain the NaVO electrode. Finally, the electrodes were punched into discs with a diameter of 14 mm to serve as cathodes for full cells.

Physical characterizations

The surface and cross section morphologies of the Zn deposits were examined by scanning electron microscopy (SEM, ZEISS Sigma 360, Germany). The phase composition of the Zn deposits and the intensity variations of different crystal planes were characterized by X-ray diffraction (XRD, PANalytical, The Netherlands). To evaluate the adsorption of DBP

on the Zn surface, X-ray photoelectron spectroscopy (XPS, AXIS Ultra DLD) was employed to analyze the chemical bonding and elemental valence states on the surface of the Zn deposits. The binding energies were calibrated using the C 1s peak at 284.8 eV as a reference. Fourier transform infrared spectroscopy (FTIR) was used to characterize the chemical structure of the Zn surface, providing additional evidence for the adsorption of DBP. The ion concentrations in the electrolyte after immersing the cathode were determined by inductively coupled plasma optical emission spectroscopy (ICP OES, 5100 SVDV, Agilent).

Electrochemical characterizations

All electrode disks were assembled into CR2032 coin cells along with Whatman glass fiber separators for electrochemical testing.

The following tests were carried out on an electrochemical workstation (CS2350, CORRTEST). The desolvation energy of Zn ions was measured by electrochemical impedance spectroscopy (EIS) using Zn||Zn symmetric cells. The measurements were conducted separately at 30, 40, 50, 60, and 70 °C, with one test performed at each temperature. The impedance range was set from 10^{-2} to 10^{5} Ω with an AC amplitude of 10 mV. The Zn^{2+} transference number was determined according to the typical Evans method. The measurement procedure involved an initial EIS measurement, followed by chronoamperometric polarization at a constant potential of 20 mV for 4000 s, and a subsequent EIS measurement[1]:

$$t_{Zn^{2+}} = \frac{I_S(\Delta V - I_0 R_0)}{I_0(\Delta V - I_S R_S)}$$

where I_0/I_S and R_0/R_S represent the initial/final current density and charge transfer resistance before and after the polarization test, and ΔV (20 mV) is the constant polarization potential for the chronoamperometry (CA) test. The EDLC value was determined by cyclic voltammetry within a potential window of -15 to 15 mV at scan rates of 6, 8, 10, 12, 14, and 16 mV s^{-1}. The Tafel curves were obtained by linear sweep voltammetry over a potential range of -0.1 to 0.1 V at a scan rate of 1 mV s^{-1}.

The CV curves were recorded using Zn||Cu half cells by cyclic voltammetry over a potential range of -0.2 to 0.5 V at a scan rate of 5 mV s^{-1}. The LSV curves were obtained by linear sweep voltammetry over a potential range of -0.4 to 0 V at a scan rate of 10 mV s^{-1}. The nucleation–growth behavior of zinc was investigated by CA using a three-electrode configuration, in which Zn served as the working electrode, Pt as the counter electrode, and a saturated calomel electrode as the reference electrode, with 1 M Na_2SO_4 + 0.1 M $ZnSO_4$ as

the electrolyte and an applied overpotential of -0.24 V.[2]

The following tests were conducted using an electrochemical testing station (CT-4008, NEWARE). The cycling stability and rate performance of Zn||Zn symmetric cells, Zn||Cu half cells, and Zn||NaV_3O_8 full cells (0.3-1.6 V) were evaluated by galvanostatic charge–discharge measurements. The Sand's time was determined by galvanostatic discharge of Zn||Zn symmetric cells at current densities of 1, 2, 3, 5, and 10 mA cm^{-2}, respectively.

Density Functional Theory (DFT) calculations

All density functional theory (DFT) calculations[3, 4] were carried out in the Vienna ab initio simulation package (VASP) based on the plane-wave basis sets with the projector augmented-wave method.[5, 6] The exchange-correlation potential was treated by using a generalized gradient approximation (GGA) with the Perdew-Burke-Ernzerhof (PBE) parametrization.[7] The van der Waals correction of Grimme's DFT-D3 model was also adopted.[8] A vacuum region of about 15 Å was applied to avoid the interaction between adjacent images. The energy cutoff was set to be 450 eV. The Brillouin-zone integration was sampled with a Γ-centered Monkhorst-Pack mesh of 2×2×1. The structures were fully relaxed until the maximum force on each atom was less than 0.02 eV/Å, and the energy convergent standard was 10^{-5} eV.

The adsorption energy Eads can be defined as, $E_{ads}=E_{*M}-E_{*}-E_{M}$, where E_{*M} stands for the energy of the monolayer with the adsorbed DBP molecule, E_{*} is the energy of surface, and E_{M} is the energy of a DBP molecule under vacuum.

Supporting Figures (Figures S1-S13)

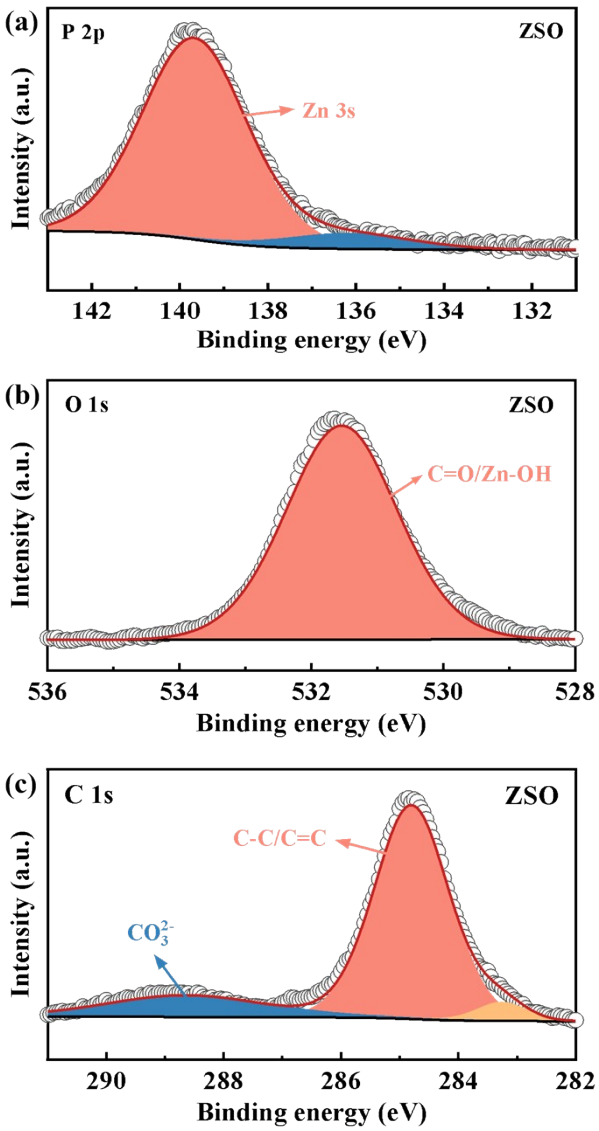

Figure S1. High-resolution XPS spectra of (a) P 2p, (b) O 1s, and (c) C 1s for the Zn deposits formed in the ZSO electrolyte.

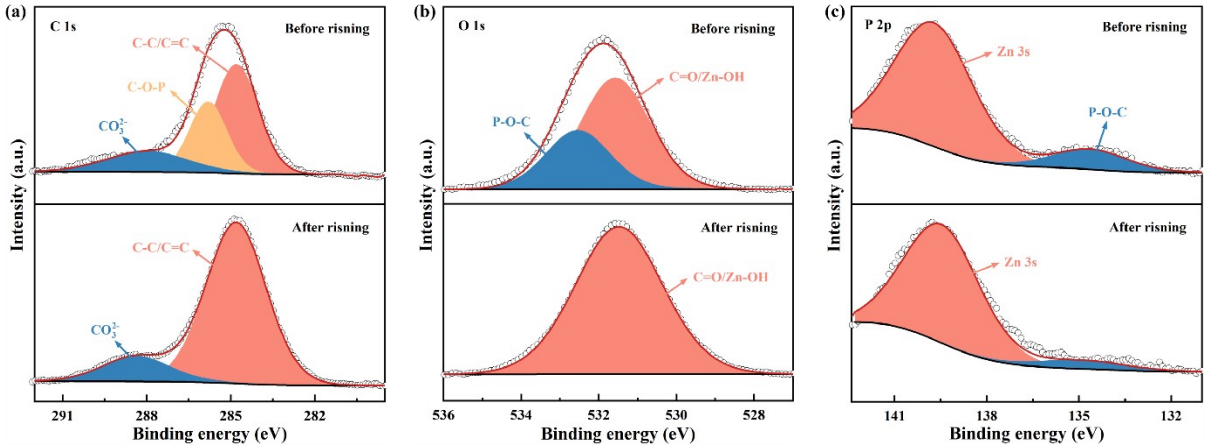

Figure S2. Comparison of high-resolution XPS spectra of (a) C 1s, (b) O 1s, and (c) P 2p for the Zn deposits cycled in the ZSO+DBP electrolyte before and after rinsing with anhydrous ethanol.

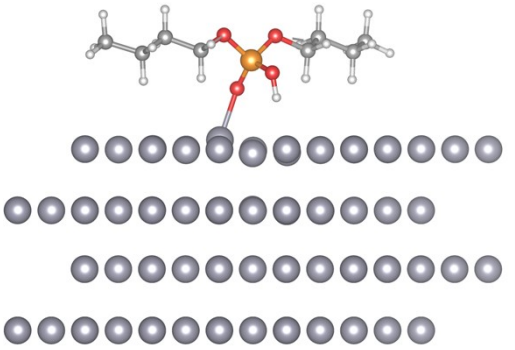

-1.15 eV

Figure S3. Adsorption energies of the P-O group on various Zn (002) crystal facets.

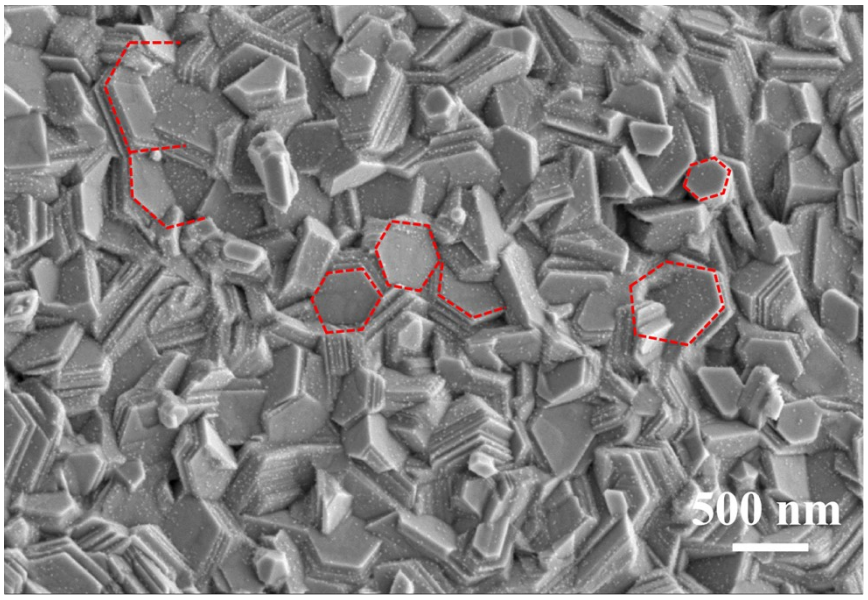

Figure S4. High-magnification SEM images of Zn deposits obtained in ZSO+DBP electrolyte at 1 mA cm^{-2} for 90 min.

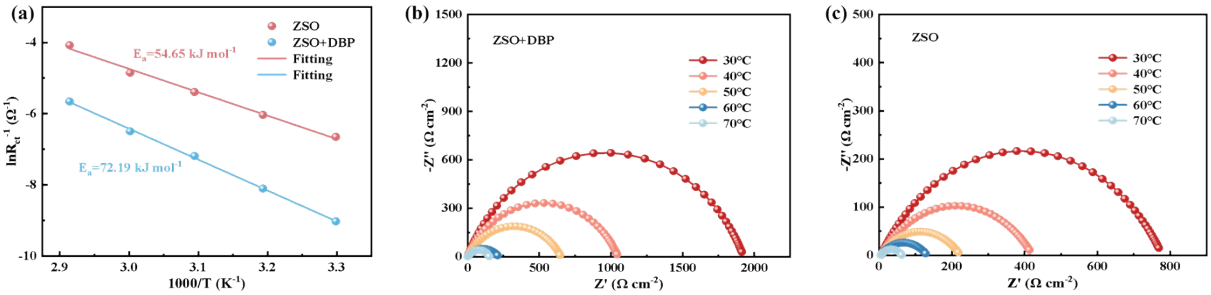

Figure S5. (a) The desolvation activation energy that was calculated according to the Arrhenius equation and the corresponding EIS curves of Zn||Zn symmetric cells at different temperatures in (b) ZSO and (c) ZSO+DBP electrolytes.

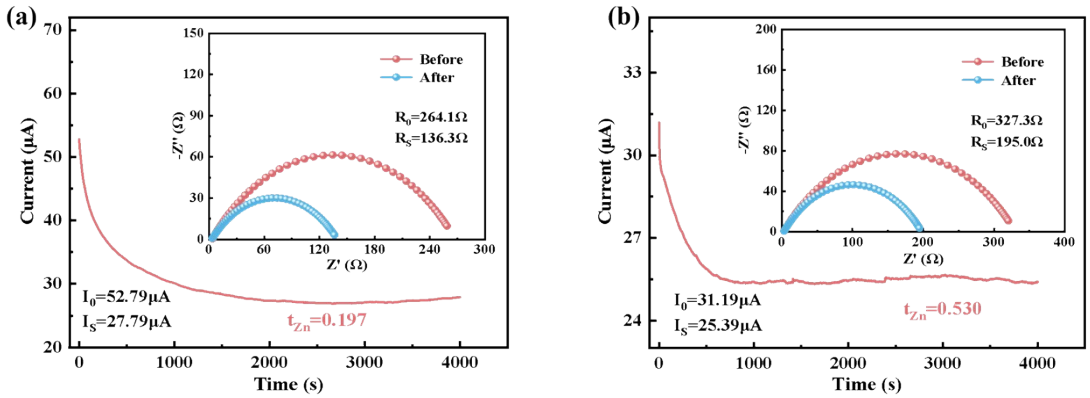

Figure S6. CA and EIS curves to calculate Zn ions transference number in (a) ZSO and (b) ZSO+DBP electrolytes.

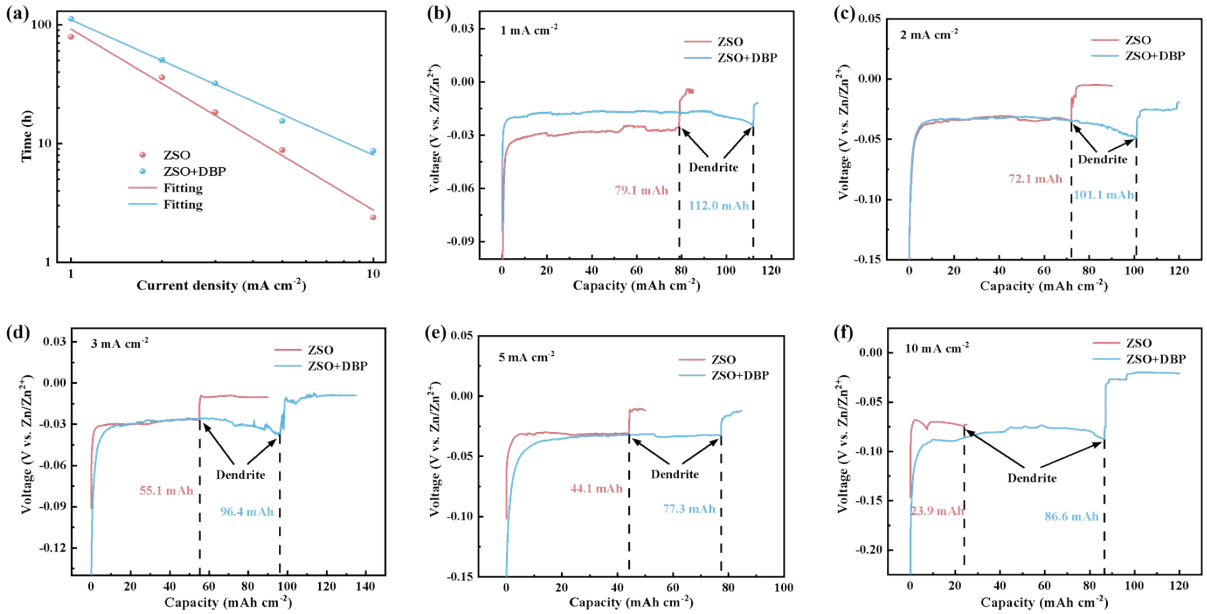

Figure S7. (a) Current-dependent Sand's time. Voltage-capacity curves of single Zn deposition at (b) 1 mA cm^{-2}, (c) 2 mA cm^{-2}, (d) 3 mA cm^{-2}, (e) 5 mA cm^{-2} and (f) 10 mA cm^{-2}.

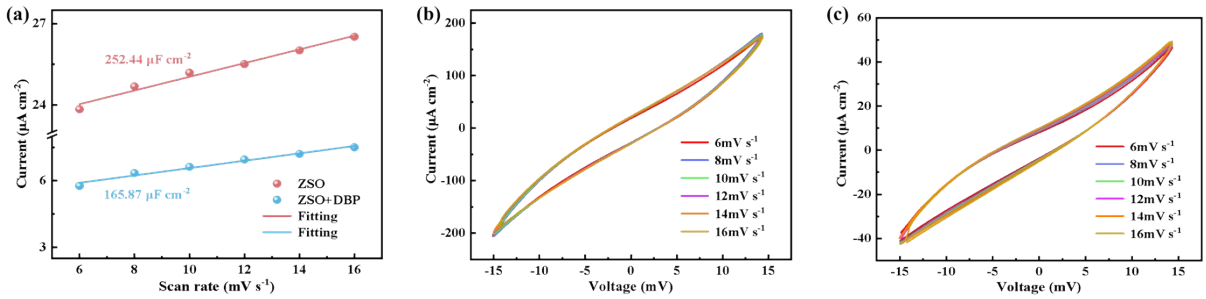

Figure S8. (a) EDLC for zinc substrates and the corresponding CV curves of Zn||Zn symmertic cells in (b) ZSO and (c) ZSO+DBP electrolytes.

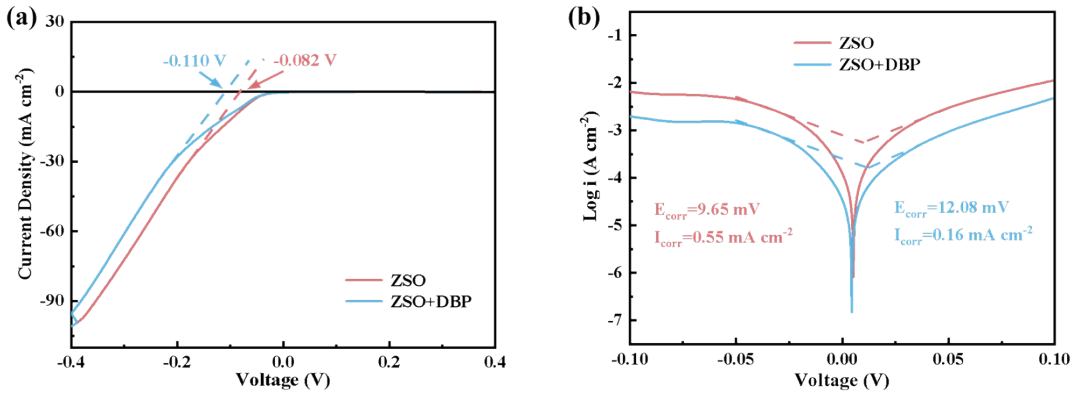

Figure S9. (a) Linear sweep voltammetry (LSV) curves and (b) Tafel curves of ZSO and ZSO+DBP electrolytes.

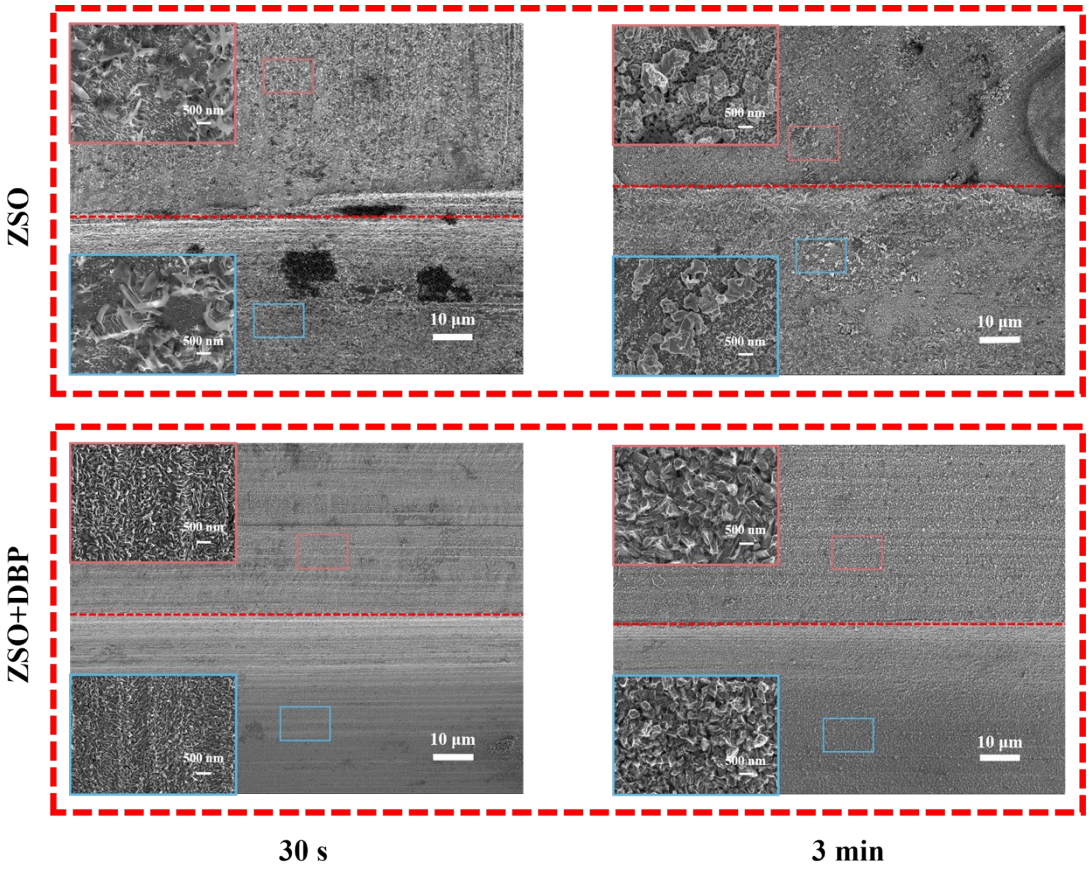

Figure S10. Morphological evolution of Zn foils with macroscopic scratches in ZSO and ZSO+DBP electrolytes at 30 s and 3 min.

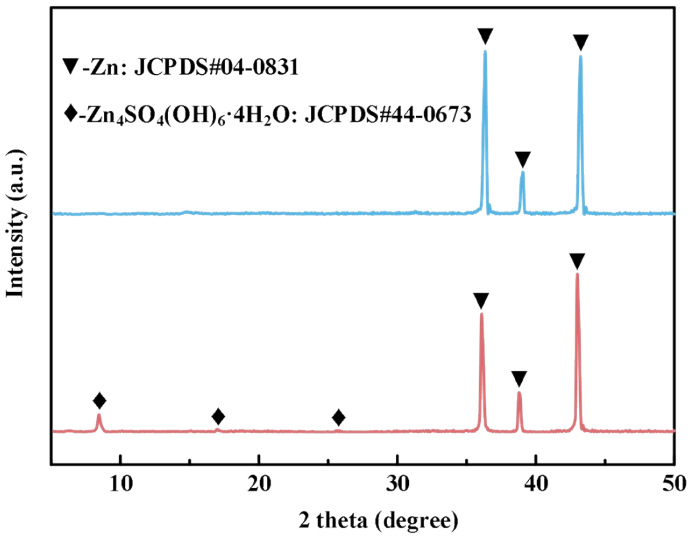

Figure S11. XRD patterns of the zinc anodes collected after cycling in ZSO and ZSO+DBP electrolytes.

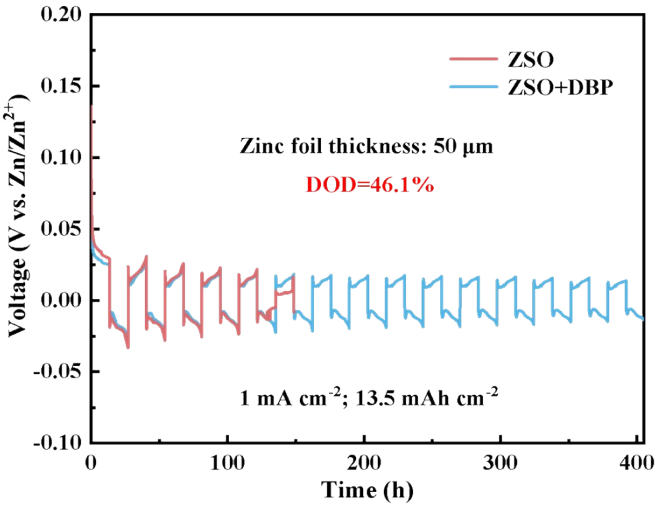

Figure S12. Long-cycling of Zn||Zn symmetric cells at 1 mA cm^{-2} and 13.5 mAh cm^{-2} (DOD = 46.1%).

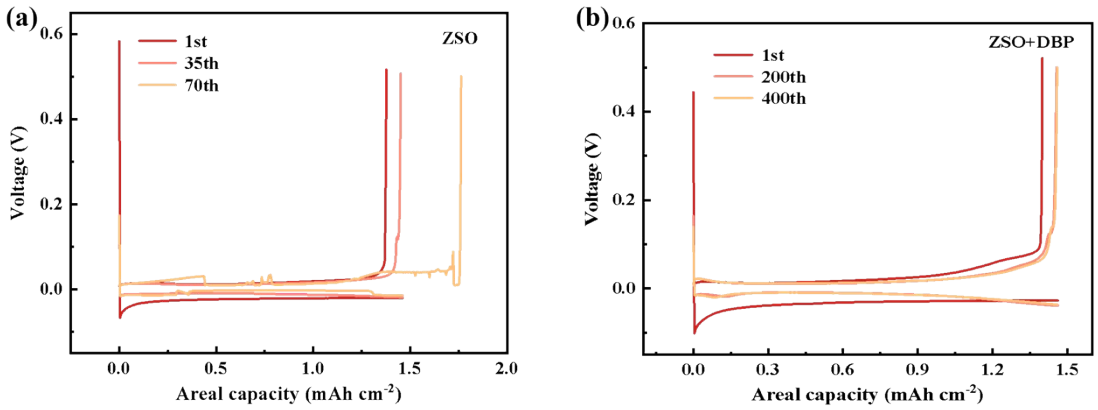

Figure S13. The time−voltage profiles of Zn||Cu cells under the condition of 0.5 mA cm^{-2} and 1.5 mAh cm^{-2} in (a) ZSO and (b) ZSO+DBP electrolytes.

References

1. L. Chang, S. Bi, J. Li, Q. Sun, X. Lu and H. Cheng, *ACS Nano*, 2025, **19**, 27424-27439.
2. Q. Zou, Z. Liang, W. Wang, D. Dong and Y.-C. Lu, *Energy & Environmental Science*, 2023, **16**, 6026-6034.
3. P. Hohenberg and W. Kohn, *Physical Review*, 1964, **136**, B864-B871.
4. W. Kohn and L. J. Sham, *Physical Review*, 1965, **140**, A1133-A1138.
5. J. F. l. G. Kresse, *Physical Review B*, 1996, **54**, 11169-11186.
6. P. E. Blöchl, *Physical Review B*, 1994, **50**, 17953-17979.
7. K. B. John P. Perdew, * Matthias Ernzerhof, *Physical Review Letters*, 1996, **77**, 3865-3868.
8. S. Grimme, J. Antony, S. Ehrlich and H. Krieg, *The Journal of Chemical Physics*, 2010, **132**, 154104.